Published in final edited form as:
Nucl Med Biol. 2012 October ; 39(7): 933–943. doi:10.1016/j.nucmedbio.2012.03.007.

Synthesis and evaluation of ^{18}F labeled alanine derivatives as potential tumor imaging agents

Limin Wang[a], **Zhihao Zha**[a], **Wenchao Qu**[a], **Hongwen Qiao**[a], **Brian P. Lieberman**[a], **Karl Plössl**[a], and **Hank F. Kung**[a,b,*]

[a]Department of Radiology, University of Pennsylvania, Philadelphia, PA 19104, USA

[b]Department of Pharmacology, University of Pennsylvania, Philadelphia, PA 19104, USA

Abstract

Introduction—This paper reports the synthesis and labeling of ^{18}F alanine derivatives. We also investigate their biological characteristics as potential tumor imaging agents mediated by alanine-serine-cysteine preferring (ASC) transporter system.

Methods—Three new ^{18}F alanine derivatives were prepared from corresponding tosylate-precursors through a two-step labelling reaction. In vitro uptake studies to evaluate and to compare these three analogs were carried out in 9L glioma and PC-3 prostate cancer cell lines. Potential transport mechanisms, protein incorporation and stability of 3-(1-[^{18}F]fluoromethyl)-L-alanine (L[^{18}F]FMA) were investigated in 9L glioma cells. Its biodistribution was determined in a rat-bearing 9L tumor model. PET imaging studies were performed on rat bearing 9L glioma tumors and transgenic mouse carrying spontaneous generated M/tomND tumor (mammary gland adenocarcinoma).

Results—New ^{18}F alanine derivatives were prepared with 7–34% uncorrected radiochemical yields, excellent enantiomeric purity (>99%) and good radiochemical purity (>99%). In vitro uptake of the L-[^{18}F]FMA in 9L glioma and PC-3 prostate cancer cells was higher than those observed for other two alanine derivatives and [^{18}F]FDG in first 1 h. Inhibition of cell uptake studies suggested that L-[^{18}F]FMA uptake in 9L glioma was predominantly via transport system ASC. After entering into cells, L-[^{18}F]FMA remained stable and was not incorporated into protein within 2 h. In vivo biodistribution studies demonstrated that L-[^{18}F]FMA had relatively high uptake in liver and kidney. Tumor uptake was fast, reaching a maximum within 30 min. The tumor-to-muscle, tumor-to-blood and tumor-to-brain ratios at 60 min post injection were 2.2, 1.9 and 3.0, respectively. In PET imaging studies, tumors were visualized with L-[^{18}F]FMA in both 9L rat and transgenic mouse.

Conclusion—L-[^{18}F]FMA showed promising properties as a PET imaging agent for up-regulated ASC transporter associated with tumor proliferation.

Keywords

^{18}F; alanine derivatives; amino acids; PET; alanine-serine-cysteine preferring amino acid transporter; ASC; Tumor imaging

CORRESPONDING AUTHOR ADDRESS: Hank F. Kung, Ph.D. Department of Radiology, University of Pennsylvania, 3700 Market Street, Room 305, Philadelphia, PA 19104. Tel: (215) 662-3096, Fax: (215) 349-5035; kunghf@gmail.com.

1. Introduction

Radiolabeled amino acids are a class of promising tracers for imaging up-regulated amino acid metabolism associated with tumor proliferation. Labeled amino acids targeting small neutral amino acid transporter (ASC), one of the most commonly overexpressed amino acid transport systems in mammalian cancer cells, have been explore. A number of amino acids, labeled with positron emitting isotopes such as ^{11}C and ^{18}F, have proven to be useful in imaging brain tumors and some peripheral cancers including prostate cancer, lung cancer, head and neck cancer and neuroendocrine tumors. Because of their low uptake in normal brain and inflammatory tissue, small amino acid based imaging agents may have improved sensitivity and specificity for brain tumor imaging over the most commonly used oncologic PET tracer, 2-[^{18}F]fluoro-2-deoxy-D-glucose (FDG).

Altered tumor metabolism facilitating the uptake and incorporation of amino acids into protein is needed to support the rapid growth and proliferation of cancer cells. Increased amino acid transport plays a major role in tumor uptake of most amino acid tracers, especially non-natural amino acids. Amino acids are transported across the cell membrane mainly through specific membrane associated carrier proteins. They are classified depending on the substrate specificity, transport mechanism and regulatory apparatus. More than 20 amino acid transport systems have been identified and characterized at the molecular level. Among these, neutral amino acid transport system A (alanine preferring), ASC (alanine-serine-cysteine preferring) and L (leucine preferring) are the most commonly up-regulated transporters in mammalian cancer cells and they are responsible for the increased amino acid metabolism in malignant tumors.

In the past few decades, system L amino acid transport substrates, which mainly consist of large and branched neutral amino acids, have been the major focus of the development of amino acid based tumor imaging agents. A number of amino acids targeting system L have demonstrated promising clinical utility, including most widely used radiolabeled amino acid: [^{11}C]methionine (MET) and many aromatic amino acid tracers such as 3-[123I]iodo-α-methyl-L-tyrosine (IMT), O-(2-[^{18}F]-fluoroethyl)-L-tyrosine (FET) and 6-[^{18}F]-fluoro-l-3,4-dihydroxyphenylalanine (FDOPA). System A substrates, [11C]α-methylamino isobutyric acid (MeAIB) and [11C]aminoisobutyric acid (AIB), were also reported. However, amino acids targeting system ASC as tumor imaging agents remain largely unexploited. Recently, 3-[^{18}F]fluoro-cyclobutyl-1-carboxylic acid (FACBC), primarily a system ASC substrate, has shown promising results for detecting glioma and prostate cancer in patients.

System ASC, in particular its subtype ASCT2, is closely associated with tumor growth and proliferation. Enhanced ASCT2 expression has been found in a variety of tumors including breast, colon and prostate cancer. This overexpression may confer survival advantage to cancer cells. Targeting system ASC could serve as a new and effective cancer therapy. Our goal is to develop novel amino acid tracers targeting system ASC that can provide useful clinical information on tumor proliferation. Sodium dependent system ASC has a broad substrate selectivity, primarily transports small and neutral amino acids, such as alanine, serine and cysteine, across cell membrane. Reported herein, we describe synthesis, radiolabeling and biological evaluation of three ^{18}F alanine derivatives with a short alkyl chain (Fig.1): 3-(1-[^{18}F]fluoromethyl)-L-alanine (L[^{18}F]FMA), 3-(1-[^{18}F]fluoromethyl)-D-alanine (D-[^{18}F]FMA), and 3-(2-[^{18}F]fluoroethyl)-L-alanine (L-[^{18}F]FEA). By a comparative evaluation of L- and D-[^{18}F]FMA, we evaluated the effects of C2 enantiomeric property on biological activities. By examining the differences between the L-[^{18}F]FMA and L-[^{18}F]FEA, we tested the affect of alkyl chain length on tumor uptake.

2. Materials and methods

2.1. General

All chemicals were purchased from Aldrich Chemical (St. Louis, MO). The commercially available materials were used without further purification unless otherwise indicated. Solvents were dried through a molecular sieve system (Pure Solve Solvent Purification System; Innovative Technology, Inc.). ^{1}H spectra and ^{13}C NMR were recorded on a Bruker DPX spectrometer at 200 MHz and 50 MHz respectively and referenced to NMR solvents as indicated. Chemical shifts are reported in ppm (δ), coupling constant *J* in Hz. The multiplicity is defined by s (singlet), d (doublet), t (triple), br (broad), and m (multiplet). High-resolution mass spectrometry (HRMS) data were obtained with an Agilent (Santa Clara, CA) G3250AA LC/MSD TOF system. Thin-layer chromatography (TLC) analyses were performed using Merck (Darmstadt, Germany) silica gel 60 F_{254} plates. Crude compounds generally were purified by flash column chromatography (FC) packed with silica gel (Aldrich). [^{18}F]Fluoride was purchased from IBA Molecular (Somerset, NJ) as an ^{18}O-enriched aqueous solution of [^{18}F]fluoride. Solid-phase extraction (SPE) cartridges such as Sep-Pak QMA Light and Oasis HLB cartridges were purchased from Waters (Milford, MA). High performance liquid chromatography (HPLC) was performed on an Agilent 1100 series system. ^{18}F radioactivity was measured by a gamma counter (Cobra II auto-gamma counter D5003 spectrometer, Perkin-Elmer). All animal experiments were carried out in compliance with ethics and animal welfare according to regulation requirements approved by Institutional Animal Care and Use Committee (University of Pennsylvania).

2.2 Chemistry

2.2.1 (S)- and (R)- 4-Benzyl 1-tert-butyl 2-(tert-butoxycarbonylamino)succinate (2)—Compound (*S*)- or (*R*)-**1** (1.0 equiv) was dissolved in CH_2Cl_2 in a round bottom flask. To this solution tert-butyl 2,2,2-trichloroacetamidate (2.0 equiv) and BF_3•Et_2O (0.1 equiv) were added. After stirring at room temperature (rt) for 2 h, the reaction mixture was cooled in an ice bath and solid $NaHCO_3$ (3.0 equiv) was added in one portion. This mixture was stirred for 10 min and filtered through a silica plug. The filtrate was evaporated in vacuo and the residue was purified by FC (EtOAc/Hexanes, 15/85, v/v) to provide (*S*)- or (*R*)-**1** as a white solid. (*S*)-**1** (Yield: 97%): $[\alpha]^{25}_D$ = - 8.1 (*c* = 2.0, MeOH). ^{1}H NMR (200 MHz, $CDCl_3$) δ 7.35 (s, 5H), 5.45 (d, 1H, *J* = 8.0 Hz), 5.13 (d, 2H, *J* = 2.6 Hz), 4.46 (pentet, 1H, *J* = 4.4 Hz), 3.00 (dd, 1H, J_1 = 16.8 Hz, J_2 = 4.6 Hz), 2.83 (dd, 1H, J_1 = 16.8 Hz, J_2 = 4.8 Hz), 1.45 (s, 9H), 1.42 (s, 9H). HRMS calcd for $C_{20}H_{29}NO_6Na$ $(M + Na)^+$: 402.1893, found: 402.1886. (*R*)-**1** (Yield: 99%): $[\alpha]^{25}_D$ = + 7.5 (*c* = 1.03, MeOH). ^{1}H NMR (200 MHz, $CDCl_3$) δ 7.35 (s, 5H), 5.45 (d, 1H, *J* = 8.0 Hz), 5.13 (d, 2H, *J* = 2.6 Hz), 4.46 (pentet, 1H, J = 4.4 Hz), 3.00 (dd, 1H, J_1 = 16.8 Hz, J_2 = 4.6 Hz), 2.83 (dd, 1H, J_1 = 16.8 Hz, J_2 = 4.8 Hz), 1.45 (s, 9H), 1.42 (s, 9H). HRMS calcd for $C_{20}H_{29}NO_6Na$ $(M + Na)^+$: 402.1893, found: 402.1886.

2.2.2. (S)- and (R)-4-tert-Butoxy-3-(tert-butoxycarbonylamino)-4-oxobutanoic acid (3)—A mixture of the ester (*S*)- or (*R*)-**2** and 10% Pd/C in absolute EtOH was shaken with hydrogen at 50 psi for 3 h. This mixture was then filtered and the filtrate was concentrated under vacuum to give product (*S*)- or (*R*)-**3** as white crystalline solid. (*S*)-**3** (Yield: 100%): $[\alpha]^{25}_D$ = − 23.6 (*c* = 1.5, MeOH). ^{1}H NMR (200 MHz, $CDCl_3$) *δ* 10.33 (brs, 1H), 5.48 (d, 1H, *J* = 8.0 Hz), 4.45 (t, 1H, *J* = 4.0 Hz), 3.02 (dd, 1H, J_1 = 17.0 Hz, J_2 = 4.0 Hz), 2.81 (dd, 1H, J_1 = 17.2 Hz, J_2 = 4.6 Hz), 1.45 (s, 18H). HRMS calcd for $C_{13}H_{23}NO_6Na$ $(M + Na)^+$: 312.1423, found: 312.1420. (*R*)-**3** (Yield: 90%): $[\alpha]^{25}_D$ = + 25.1 (*c* = 1.03, MeOH). ^{1}H NMR (200 MHz, $CDCl_3$) *δ* 10.33 (brs, 1H), 5.48 (d, 1H, *J* = 8.0 Hz), 4.45 (t, 1H, *J* = 4.0 Hz), 3.02 (dd, 1H, J_1 = 17.0 Hz, J_2 = 4.0 Hz), 2.81 (dd, 1H, J_1 = 17.2 Hz, J_2 =

4.6 Hz), 1.45 (s, 18H). HRMS calcd for $C_{13}H_{23}NO_6Na$ $(M + Na)^+$: 312.1423, found: 312.1420.

2.2.3. Reduction reaction for synthesis of 5 and 6—Corresponding acid **3** or **4** (1.0 equiv) was dissolved in THF in a round bottom flask and the solution was cooled to −10 °C. To this solution Et_3N (1.1 equiv) and ethyl chloroformate (1.1 equiv) were added dropwise. After stirring at −10 to −5 °C for 30 min, the reaction mixture was filtered off. To a mixture of $NaBH_4$ (2.2 equiv) in H_2O in a two-neck flask cooled with an ice bath, the above filtrate was added slowly. The mixture was stirred at rt for additional 4 h and was then acidified with 1 M HCl under cooling with a ice bath until pH reached 2 – 3. The water phase was extracted with EtOAc. The organic phases were collected and combined, washed with saturated $NaHCO_3$ and brine, and dried with $MgSO_4$. The filtrate was evaporated *in vacuo* and the residue was purified by FC to afford alchohol **5** or **6**.

2.2.3.1 (S)-tert-Butyl 2-(tert-butoxycarbonylamino)-4-hydroxybutanoate ((S)-5): Yield: 87%. FC (EtOAc/Hexanes, 35/65 to 45/55, v/v). $[\alpha]^{25}_D = -39.3$ ($c = 1.03$, EtOH). ^{1}H NMR (200 MHz, $CDCl_3$) δ 5.35 (brs, 1H), 4.36 (brs, 1H), 3.57–3.77 (m, 2H), 2.92 (brs, 1H), 2.05–2.20 (m, 2H), 1,48 (s, 9H), 1.45 (s, 9H). HRMS calcd for $C_{13}H_{25}NO_5Na$ $(M + Na)^+$: 298.1630, found: 298.1632.

2.2.3.2 (R)-tert-Butyl 2-(tert-butoxycarbonylamino)-4-hydroxybutanoate ((R)-5): Yield: 82%. FC (EtOAc/Hexanes, 35/65 to 45/55, v/v). $[\alpha]^{25}_D = +43.3$ ($c = 0.99$, MeOH). ^{1}H NMR (200 MHz, $CDCl_3$) δ 5.35 (brs, 1H), 4.36 (brs, 1H), 3.57–3.77 (m, 2H), 2.92 (br s, 1H), 2.05–2.20 (m, 2H), 1,48 (s, 9H), 1.45 (s, 9H). HRMS calcd for $C_{13}H_{25}NO_5Na$ $(M + Na)^+$: 298.1630, found: 298.1632.

2.2.3.3 (S)-tert-butyl 2-(tert-butoxycarbonylamino)-5-hydroxypentanoic acid (6): Yield: 94%. FC (EtOAc/Hexanes, 30/70 to 45/55, v/v). $[\alpha]^{23}_D = -23.6$ ($c = 1.05$, EtOH).^{1}H NMR (200 MHz, $CDCl_3$): 5.13 (brs, 1 H), 4.21 (brs, 1 H), 3.69 (quartet, 2 H, $J = 5.6$ Hz), 1.89-1.61 (m, 4 H), 1.48 (s, 9 H), 1.45 (s, 9 H).^{13}C NMR (50 MHz, $CDCl_3$): 172.1, 155.7, 81.9, 79.8, 62.0, 53.8, 29.6, 28.4, 28.1. HRMS calcd for $C_{14}H_{27}NaNO_5$ $(M + Na)^+$: 312.1787, found: 312.1776.

2.2.4. Tosylation reaction for synthesis of 7 and 8—Corresponding alcohol **5** or **6** (1.0 equiv) was dissolved in CH_2Cl_2 in a round bottom flask. To this solution toluenesulfonyl chloride (2.0 equiv), Et_3N (5.0 equiv) and DMAP (0.1 equiv) were added. The mixture was stirred at rt for 1 h. After reaction, the mixture was washed with H_2O and brine, and then dried with $MgSO_4$. The filtrate was evaporated *in vacuo* and the residue was purified by FC.

2.2.4.1 (S)-tert-butyl 2-(tert-butoxycarbonylamino)-4-(tosyloxy)butanoate ((S)-7): Yield: 90%. FC (EtOAc/Hexanes, 20/80, v/v). $[\alpha]^{25}_D = -16.7$ ($c = 1.09$, MeOH). ^{1}HNMR ($CDCl_3$) δ: 7.80 (d, 2H, $J = 8.4$ Hz), 7.26 (d, 2H, $J = 8.4$ Hz), 5.01 (brs, 1H), 4.06–4.18 (m, 3H), 2.46 (s, 3H), 2.05–2.27(m, 2H), 1.46 (s, 9H), 1.42 (s, 9H). HRMS calcd for $C_{20}H_{35}N_2O_7S$ $(M + NH_4)^+$: 447.2165, found: 447.2173.

2.2.4.2 (R)-tert-butyl 2-(tert-butoxycarbonylamino)-4-(tosyloxy)butanoate ((R)-7): Yield: 83%. FC (EtOAc/Hexanes, 20/80, v/v). $[\alpha]^{25}_D = +16.2$ ($c = 1.03$, MeOH). ^{1}HNMR ($CDCl_3$) δ: 7.80 (d, 2H, $J = 8.4$ Hz), 7.26 (d, 2H, $J = 8.4$ Hz), 5.01 (brs, 1H), 4.06–4.18 (m, 3H), 2.46 (s, 3H), 2.05–2.27(m, 2H), 1.46 (s, 9H), 1.42 (s, 9H). HRMS calcd for $C_{20}H_{35}N_2O_7S$ $(M + NH_4)^+$: 447.2165, found: 447.2173.

2.2.4.3 (S)-tert-butyl 2-(tert-butoxycarbonylamino)-5-(tosyloxy)pentanoic acid (8): Yield: 86%. FC (EtOAc/hexanes, 2/8, v/v). $[\alpha]^{23}_D = -11.8$ (c = 1.0, EtOH). ^{1}H NMR (200 MHz, $CDCl_3$): 7.79 (d, 2 H, J = 8.1 Hz), 7.35 (d, 2 H, J = 8.1 Hz), 5.01 (d, 1 H, J = 6.6 Hz), 4.18-4.01 (m, 3 H), 2.46 (s, 3 H), 1.87-1.62 (m, 4 H), 1.46 (s, 9 H), 1.43 (s, 9 H). ^{13}C NMR (50 MHz, $CDCl_3$): 171.5, 155.4, 144.9, 133.2, 130.0, 128.0, 82.3, 79.9, 70.0, 53.5, 29.2, 28.4, 28.1, 25.1, 21.8. HRMS calcd for $C_{21}H_{34}NO_7S$ $(M + H)^+$: 444.2056, found: 444.2056.

2.2.5. (S)-tert-butyl 2-(tert-butoxycarbonylamino)-5-Iodopentanoic acid (9)—A mixture of tosylate **8** (0.798 g, 1.80 mmol) and NaI (0.600 g, 4.0 mmol) in acetone (10 mL) was stirred at 60 °C for 3.5 h. The reaction mixture was cooled to rt and then filtered. The filtrate was concentrated and submitted to FC (EtOAc/hexanes, 15/85, v/v) to give light yellow oil **9** (0.554 g, 77%): $[\alpha]^{24}_D = -19.2$ (c = 1.0, MeOH). ^{1}H NMR (200 MHz, $CDCl_3$): 5.12 (d, 1 H, J = 7.2 Hz), 4.19-4.08 (m, 1 H), 3.30-3.12 (m, 2 H), 1.99-1.65 (m, 4 H), 1.49 (s, 9 H), 1.45 (s, 9 H); ^{13}C NMR (50 MHz, $CDCl_3$): 171.6, 155.4, 82.3, 79.9, 53.2, 34.0, 29.3, 28.5, 28.2, 5.9. HRMS calcd for $C_{14}H_{26}INO_4Na$ $(M + Na)^+$: 422.0804, found: 422.0802.

2.2.6. Fluorination reaction for synthesis of 10 and 11—To a stirred solution of tris(dimethylamino)sulfonium difluorotrimethylsilicate (5.0 equiv) in CH_2Cl_2/THF (1/1) was added dropwise $Et_3N{\cdot}(HF)_3$ followed by tosylate **7** or **8** (1.0 equiv) in THF. The mixture was heated to 45 to 50 °C by oil bath overnight. Upon completion of reaction, the oil bath was removed, the reaction mixture was diluted with EtOAc and washed with half saturated $NaHCO_3$, water and brine subsequently. The EtOAc phase was collected, dried over $MgSO_4$, filtered, concentrated in *vacuo*. The residue was purified by FC (EtOAc/Hexanes, 25/75 to 40/60, v/v) to provide fluoride **10** or **11**.

2.2.6.1 (S)-tert-Butyl 2-(tert-butoxycarbonylamino)-4-fluorobutanoate ((S)-10): Yield: 86%. FC (EtOAc/Hexanes, 10/90, v/v). $[\alpha]^{25}_D = -40.5$ (c = 1.04, MeOH). ^{1}HNMR ($CDCl_3$) d: 5.18 (brs, 1H), 4.67 (t, 1H, J = 5.2 Hz), 4.44 (t, 1H, J = 5.6 Hz), 4.21–4.32 (m, 1H), 2.06–2.28 (m, 2H), 1.48(s, 9H), 1.46 (s, 9H). HRMS calcd for $C_{13}H_{24}FNO_4Na$ $(M + Na)^+$: 300.1587, found: 300.1593.

2.2.6.2 (R)-tert-Butyl 2-(tert-butoxycarbonylamino)-4-fluorobutanoate ((R)-10): Yield: 86%. FC (EtOAc/Hexanes, 10/90, v/v). $[\alpha]^{25}_D = +38.1$ (c = 1.04, MeOH). ^{1}HNMR ($CDCl_3$) δ: 5.18 (brs, 1H), 4.67 (t, 1H, J = 5.2 Hz), 4.44 (t, 1H, J = 5.6 Hz), 4.21–4.32 (m, 1H), 2.06–2.28 (m, 2H), 1.48(s, 9H), 1.46 (s, 9H). HRMS calcd for $C_{13}H_{24}FNO_4Na$ $(M + Na)^+$: 300.1587, found: 300.1593.

2.2.6.3 (S)-tert-butyl 2-(tert-butoxycarbonylamino)-5-Fluoropentanoic acid (11): Yield: 67%. FC (EtOAc/Hexanes, 25/75 to 40/60, v/v). $[\alpha]^{25}_D = -28.2$ (c = 1.0, EtOH). ^{1}H NMR (200 MHz, $CDCl_3$) δ 5.07 (d, 1 H, J = 7.8 Hz), 4.58 (t, 1 H, J = 5.6 Hz), 4.35 (t, 1 H, J = 5.6 Hz), 4.21 (brs, 1 H), 1.95-1.68 (m, 4 H), 1.48 (s, 9 H), 1.45 (s, 9 H). ^{13}C NMR (50 MHz, $CDCl_3$) δ 171.8, 155.5, 85.2, 82.2, 81.9, 79.9, 53.7, 29.1, 29.0, 28.5, 28.2, 26.7, 26.3. HRMS calcd for $C_{14}H_{26}FNO_4Na$ $(M + Na)^+$: 314.1744; found: 314.1741.

2.2.7. Deprotection reaction for synthesis of FMA and FEA—To a mixture of **10** or **11** (1.0 equiv) with dimethylsulfide cooled with an ice bath (0 °C), trifluoroacetic acid (TFA) was added dropwise. After addition, the ice bath was removed and the reaction was kept at rt for 2.5 h. The solution was evaporated *in vacuo* to remove most TFA. The residue was dissolved in H_2O, and washed with CH_2Cl_2 and Et_2O sequentially. The aqueous part was neutralized to pH 7 by aqueous ammonia. The neutralized solution was concentrated and the residue was recrystallized in EtOH/H_2O to provide the final product as white solid.

2.2.7.1 (S)-2-Amino-4-fluorobutanoic acid (L-FMA): Yield: 64%. $[\alpha]^{25}_{D} = -2.2$ (c = 0.49, H_2O). ^{1}HNMR (D_2O) δ: 4.57–4.64 (m, 1 H), 3.92 (dd, 1H, J_1 = 5.0 Hz, J_2= 7.2 Hz), 2.09–2.51 (m, 2H). ^{13}C NMR (50 MHz, D_2O + trace CD_3OD) δ 174.3, 84.2, 80.9, 53.2, 31.3, 30.9. HRMS calcd for $C_4H_9FNO_2$ $(M + H)^+$: 122.0617; found: 122.0613.

2.2.7.2 (R)-2-Amino-4-fluorobutanoic acid (D-FMA): Yield: 67%. $[\alpha]^{25}_{D} = +2.1$ (c = 0.51, H_2O). ^{1}HNMR (D_2O) δ: 4.57–4.64 (m, 1 H), 3.92 (dd, 1H, J_1 = 5.0 Hz, J_2 = 7.2 Hz), 2.09–2.51 (m, 2H). ^{13}C NMR (50 MHz, D_2O + trace CD_3OD) δ 174.3, 84.2, 80.9, 53.2, 31.3, 30.9. HRMS calcd for $C_4H_9FNO_2$ $(M + H)^+$: 122.0617; found: 122.0613.

2.2.7.3 (S)-2-Amino-5-Fluoropentanoic acid (L-FEA): Yield: 59%. $[\alpha]^{24}_{D} = +6.4$ (c = 0.54, H_2O); ^{1}H NMR (200 MHz, D_2O) δ 4.70 (t, 1 H, J = 5.4 Hz), 4.46 (t, 1 H, J = 5.6 Hz), 3.81 (t, 1 H, J = 6.0 Hz), 2.08-1.76 (m, 4 H); ^{13}C NMR (50 MHz, D_2O + trace CD_3OD) δ 175.5, 87.0, 83.8, 55.5, 27.7, 27.6, 26.8, 26.4. HRMS calcd for $C_5H_{11}FNO_2$ $(M + H)^+$: 136.0074; found: 136.0780.

2.3. Radiosynthesis procedure

[^{18}F]Fluoride trapped on a Sep-Pak light QMA cartridge (pre-conditioned with 10 mL 1 N $NaHCO_3$, 10 mL water and dried with N_2) was eluted with one of the following solutions: 18-Crown-6/$KHCO_3$ (0.93 mL acetonitrile and 0.17 mL water containing 8 mg 18-Crown-6 and 1.5 mg $KHCO_3$), K_{222}/K_2CO_3 (0.93 mL acetonitrile and 0.17 mL water containing 11.0 mg Kryptofix 222 and 2.0 mg K_2CO_3), or $TBAHCO_3$ (0.75 mL acetonitrile and 0.25 mL water containing 21.5 mg $TBAHCO_3$). The ^{18}F activity was dried azeotropically under N_2 at 80 °C. Five milligrams precursor in 1mL solution (CH_3CN or DMSO) was added to the dried ^{18}F and fluorination reaction continued at selected temperature for 10 to 15 min. After fluorination, 10 mL water was added to the reaction solution, and the mixture was passed through a Waters Oasis HLB cartridge (preconditioned with 10 mL ethanol and 10 mL water). The cartridge was washed with 4 mL water and then eluted with 0.5 mL CH_3CN to afford ^{18}F labeled intermediates. After removing CH_3CN under N_2 at rt, TFA was added to the intermediates, deprotection reaction continued at 60 °C for 10 min. Upon completion of deprotection, TFA was removed with N_2 flow and then 1 mL sterile water was added to formulate the final products. Chemical and radiochemical purity of the intermediates and final products were analyzed by analytical HPLC performed on a Phenomenex Gemini C-18 column (250 × 4.6 mm, 5 μ) eluted by solvent system A: CH_3CN/0.1% formic acid (60/40) at flow rate of 1mL/min. Enantiomeric purity of the intermediates was determined with a chiral OD-H column (250 × 4.6 mm, 5 μ) in solvent system B: Hexane/EtOH (96/4) at the flow rate of 0.6mL/min. Enantiomeric purity of the final products was determined with a Chirex 3126 (D)-penicillamine column (150 × 4.6 mm, 5 μ) using solvent system C: 2 mM $CuSO_4$ at flow rate of 0.5 mL/min.

2.4. Cell culture

All cell lines were purchased from ATCC (Manassas, VA). The cancer cells were cultured in the medium recommended by ATCC supplemented with 10% fetal bovine serum (Hycolne, Logan, UT) and 1% penicillin/streptomycin. For 9L and PANC-1, Dulbecco's Modified Eagle's Medium (DMEM, GIBCO BRL, Grand Island, NY) was used. For PC-3, Kaighn's Modification of Ham's F-12 Medium (ATCC) was used; For U-87 MG, Eagle's Minimum Essential Medium (EMEM, ATCC) was used. Cells were maintained in T-75 culture flask under humidified incubator conditions (37 °C, 5% CO_2) and were routinely passaged at confluence.

2.5. In vitro cell uptake studies

Tumor cells (2×10^5/well in 12-well flask) were plated in culturing media 24 h prior to studies. On the day of experiment, the media was aspirated and the cells were washed three times with phosphate buffered saline (PBS, containing of Ca^{2+} and Mg^{2+}). For cell uptake studies, ligand of choice was mixed within PBS solution and was then added to each well (37 KBq/mL/well). The cells were incubated at 37 °C for 5, 30, 60 and 120 min. At the end of the incubation period, the PBS solution containing the ligands was aspirated and then the cells were washed 3 times with 1 mL ice cold PBS without Ca^{2+} and Mg^{2+}. After washing with ice cold PBS, 350 μL 1 M NaOH was used to lyse the cells. The lysed cells were collected onto filter paper and counted together with samples of initial dose using a gamma counter (Cobra II, Perkin-Elmer). One hundred microliters of the cell lysate was used for determination of protein concentration by modified Lowry protein assay. The data was normalized as percentage uptake of initial dose relative to 100 μg protein content (% ID/100 μg protein).

2.6 Transport characterization studies

The 9L cells were processed as previously described in cell uptake studies. Selected inhibitors were added to cells together with L-[^{18}F]FMA and [^{3}H]Alanine in PBS solution and incubated for 30 min. Inhibitors included MeAIB (0.5 to 5 mM) for system A, 2-amino-bicylo[2.2.1] heptane-2-carboxylic acid (BCH, 0.5 to 5 mM) for system L, L-Serine (Ser) and L-Alanine (Ala, 0.5 to 5 mM) for system ASC and L-γ-Glutamyl-p-nitroanilide (GPNA, 0.1 to 1 mM) for system ASCT2. L-γ-Glutamyl-anilide (GA, 0.1 to 1 mM), which has low ASCT2 inhibition activity, was used as a control. Due to the limitation of solubility of GPNA and GA, maximum concentration 1 mM was used for these inhibitors. In sodium dependence studies, PBS buffer was replaced with Na^+ free solution (143 mM choline chloride, 2.68 mM KCl and 1.47 mM KH_2PO_4). In pH dependence studies, PBS solution was adjusted to desirable pH with NaOH and/or HCl solution. The data was normalized in reference to uptake of L-[^{18}F]FMA at 30 min without any inhibitors in PBS solution at pH 7.4.

2.7 In vitro metabolic stability

L-[^{18}F]FMA mixed within PBS solution was added to each well plated with 9L cells (370 KBq/mL/well). The cells were incubated at 37 °C for selected time period. At the end of the incubation period, the wells were aspirated free of ligand and then washed with ice cold PBS as described above. Cells were then detached using cell scraper and transferred into BioMasher disposable homogenizer (Omni International, Kennesaw, GA). Filtrate on BioMasher was washed with PBS twice and then sample of final homogenate solution was analyzed with HPLC (Chriex 3126 (D)-penicillamine 150 × 4.6 mm, 2 mM $CuSO_4$, 0.5 mL/min).

2.8 Protein Incorporation

The 9L cells was incubated for 30 and 120 minutes with 222 KBq L-[^{18}F]FMA and 37 KBq [^{3}H]Alanine (Perkin Elmer, MA) in 3 mL PBS. After removal of the radioactive medium, the cells were washed three times with ice cold PBS without Ca^{2+} and Mg^{2+}, treated with 0.25% trypsin and resuspended in PBS. The samples were centrifuged (13000 rpm, 5 min), the supernatant removed and the cells were suspended in 1M trichloroacetic acid (TCA) at 0 °C for 30 min. After precipitation, the cells were centrifuged again (13000 rpm, 5 min) and washed twice with 1 M ice cold TCA. The radioactivity in both supernatant and pellet was determined. Protein incorporation was calculated as percentage of acid percipitable activity. The recovery of intracellular tracer in its free from was monitored by calculating the recovery of activity added just before TCA precipitation.

2.9 Biodistribution studies with Fisher rats bearing 9L tumors

Male Fisher (F344) rats (43–49 days old) were purchased from Charles Rivers Laboratory (Malvern, PA). Tumor implantation in F344 rats was accomplished by injecting 4–5 million 9L cells/isograft. The cells suspended in PBS solution (0.2 mL) were injected subcutaneously into each of the shoulder flanks of the F344 rat. The growth of the tumor was monitored daily for two weeks. When the volume of the tumors reached ~1 cm^3, the rat tumor models were used for biodistribution or microPET imaging studies. Animals were fasted for 12–18 hours prior to the procedure. 0.2 mL Saline solution containing the tracer L-[^{18}F]FMA (~925 KBq) was injected into the lateral tail vein under isoflurane anesthesia (1–2%, 1 L/min oxygen). The animals were sacrificed at 2, 30, 60 and 120 min post-injection by cardiac excision under anesthesia. Six rats were sacrificed at each time point. The organs of interest and tumors were removed and weighed. The radioactivity in each tissue was measured using a gamma counter together with sample of the initial dose. Results were expressed as the percentage of the injected dose per gram (%ID/g) of tissue. Each value represents the mean ± SD of six rats unless otherwise noted.

2.10. Small animal imaging studies

PET imaging studies were performed on a Phillips Mosaic small animal PET scanner, which has an imaging field of view of 11.5 cm. F344 rat tumor model as described before and transgenic mice bearing M/tomND spontaneous human mammary gland tumors were used for the imaging studies. The transgenic female mice, which were bred and weigh between 20–30g, were obtained from Dr. Lewis Chodosh (Abramson Family Cancer Research Institute, PA). A doxycycline sensitive promoter genetically engineers these mice to express the myc gene. When the mice are administered doxycycline through their drinking water (2 mg/mL) the expression of the myc gene is up regulated. 0.3 mL Saline solution containing the tracer L-[^{18}F]FMA (~13 to 30 MBq) was injected into the lateral tail vein under isoflurane anesthesia (1–2%, 1 L/min oxygen). Data acquisition began immediately following the intravenous injection. Dynamic scans were conducted over a period of 2 h (5 min/frame; image voxel size 0.5 mm^3). Animals were visually monitored for breathing and a heating pad was used to maintain body temperature throughout the entire procedure. Images were reconstructed using 3D row action maximum likelihood algorithm (RAMLA). Analysis of images was performed using using AMIDE software (http://amide.sourceforge.net/). Regions of interest (ROI, such as tumor and muscle) were drawn and time-activity curves were generated from calculation of ROI for kinetic analysis.

3. Results and Discussion

3.1 Chemistry

Standard “cold” compounds L-FMA and D-FMA were synthesized from commercially available Boc-Asp(OBzl)-OH **1** (as shown in Scheme 1). After esterification of carboxylic group and removal of benzyl group via hydrogenolysis, partially protected aspartic acid derivative Boc-Asp-OtBu **3** was reduced to desired alcohol **5** following a previously reported mixed anhydride reduction method. Tosylation of alcohol **5** provided the labeling precursors in 83 to 90% yield. The fluoride intermediate **10** was prepared by following our recently developed fluorination method using a “neutralized” tris(dimethylamino)sulfonium difluorotrimethylsilicate (TASF) (mixture of TASF and $Et_3N(HF)_3$). After fluorination and then deprotection with TFA, final compounds L-FMA and D-FMA could be obtained with an overall yield of 37 to 39%. The synthesis of L-FEA started from protected partially protected glutamic acid derivative, Boc-Glu-OtBu **4** (Scheme 1). Tosylate intermediate **8** was prepared through reduction of **4** and then tosylation of alcohol **6**. The labeling precursor iodide **9** was then produced in 77% yield through the exchange of tosyl group to iodo group via Finkelstein type reaction. It is noteworthy to point out that the desirable labeled product

could not be prepared from tosylate **8**, probably due to its fast rate of cyclization in labeling process. The standard compound for radiosynthesis L-FEA was prepared from tosylate **8** after fluorination and deprotection, similar to FMA.

3.2 Radiolabeling

[^{18}F]FMA and [^{18}F]FEA were conveniently prepared via a two-step reaction — fluorination using 18-Crown-6/$KHCO_3$/K[^{18}F]F followed by deprotection in TFA. Table 1 summarizes the labeling results of the new alanine derivatives under the condition described in scheme 2, including synthesis time, non-decay corrected radiochemical yield (RCY), radiochemical purity (RCP) and enantiomeric purity.

One potential problem in labeling amino acid derivatives is the racemization occurring during radiofluorination. The L- and the D-isomer of amino acids usually display a very different biological activity. There is a great disparity in tumor cell uptake between L- and D-isomers: the naturally occurring L-isomers are more readily transported than their corresponding D-isomers. Thus, obtaining the enantiomerically pure ^{18}F labeled amino acids is important for accurate biological evaluation. To establish the optimal condition for preparing enantiomerically pure [^{18}F]FMA, we have carefully studied the conditions of fluorination for radiosynthesis of L-[^{18}F]FMA. The results demonstrated that in CH_3CN at 80 °C using 18-Crown-6 as the phase transfer catalyst and $KHCO_3$ as the base led to enantiomerically pure intermediate (*S*)-[^{18}F]**10** (*ee* >99%). In contrast, using reagents K_{222}/K_2CO_3 (*ee* 93–95%) and $TBAHCO_3$ (*ee* 79–84%) led to a lower enantiomeric purity (Fig. 2). Effects of solvent and temperature on enantiomeric purity and labeling yield were also evaluated (see Table 2). (*S*)-[^{18}F]**10** fluorinated with 18-Crown-6/$KHCO_3$/K[^{18}F]F was prepared with the highest yield and optical purity in DMSO at 80 °C. Synthesis of (*S*)-[^{18}F]**11**, the intermediate of L-[^{18}F]FEA, required lower temperature (60 °C) to reduce cyclization, a side reaction.

3.3 Cell uptake studies

To evaluate these new ^{18}F-labeled alanine derivatives, we first conducted the cell uptake studies in 9L gliosarcoma and PC-3 prostate cancer cells. The in vitro cell uptake in phosphate buffered saline (PBS) was measured at selected time points up to 2 h (Fig. 3). FDG was used as the reference since it is the most commonly used PET tracer. The results demonstrated that L[^{18}F]FMA showed the highest uptake among the three new alanine derivatives. Its uptake at 1 h is 2.4 and 1.2 fold higher than those of FDG in 9L and PC-3 cells, respectively. This observation is highly important because it suggests that amino acid transport system(s) (potentially system ASC as indicated by transport characterization studies) is capable of moving the alanine analog, L[^{18}F]FMA, across tumor membrane in a higher speed than that observed for FDG via the glucose transporter. This fast tumor cell uptake fulfills the first requirement for developing biomarker for detecting tumor proliferation.

Uptake of the D-isomer (D-[^{18}F]FMA) was very low (< 1% ID/100 g protein). Maximum uptake of D-[^{18}F]FMA was less than 5% of that of its L- isomer in both cell lines. The data suggest that the L configuration is essential for the tumor cell uptake for this series of alanine derivative. Derivative with a longer alkyl chain, L-[^{18}F]FEA, showed a faster kinetics, reaching the peak within 30 min and then washes out from the tumor cells thereafter. Maximum uptake of L-[^{18}F]FEA could only reach 26 and 63% of that of L-[^{18}F]FMA in 9L and PC-3 cells, respectively. These data suggested that among the new alanine analogs, L-[^{18}F]FMA was the most promising candidate. Its biological properties were further investigated.

In addition to 9L and PC-3 cells, uptake of L-[^{18}F]FMA in PANC-1 human pancreatic epithelial carcinoma and U-87 MG human glioma was measured, as well (Fig.4). High uptake, 25 to 60 % ID/100 μg protein at 60 min, was observed in these cancer cell lines. Although uptake value varies in different cell lines, similar kinetics was observed – uptake reached a maximum around 60 min. It is reasonable to conclude that L-[^{18}F]FMA is taken up efficiently by both fast and slow growing tumor cells.

3.4 Transport characterization studies

To examine the underlying mechanism(s) of uptake of L-[^{18}F]FMA, we have conducted a series of competitive uptake inhibition studies in 9L glioma cells. A number of inhibitors specific for system A, ASC and L were used. The uptake of L-[^{18}F]FMA was measured in absence of inhibitors as well as in the presence of concentration from ranging 0.5 to 5 mM of system A inhibitor MeAIB, system L inhibitor BCH, and system ASC inhibitors L-Ala and L-Ser. Sodium and pH dependence studies were carried out as well for better characterization of the transport system(s) responsible for uptake of L-[^{18}F]FMA. These studies were performed with a 30 min incubation time and the results were normalized to uptake of L-[^{18}F]FMA in PBS (pH 7.4) in absence of inhibitors as summarized in Fig. 5. The results showed that MeAIB had no inhibitory effect on the uptake of L-[^{18}F]FMA (Fig. 5B); This indicates system A does not contribute to its transportation across the membrane. System L inhibitor BCH could reduce L-[^{18}F]FMA's uptake up to 20%. In contrast, system ASC inhibitor L-Ala and L-Ser could reduce >95% of the uptake at 5 mM concentration (Fig. 5A). Furthermore, in Na^+ free media, uptake of L-[^{18}F]FMA was reduced by 85%. Changes in pH did not have significant effect on the uptake of L-[^{18}F]FMA (110 ± 13% and 86 ± 5% of control at pH 6 and 8, respectively), similar to L-[^{3}H]Ala (93 ± 4% and 99 ± 3% of control at pH 6 and 8, respectively). These data indicate that uptake of L-[^{18}F]FMA is predominately through a sodium dependent and pH insensitive system ASC. Sodium independent system L plays a minor role and it may be responsible for the observed sodium independent cell uptake.

We also examined the selectivity of L-[^{18}F]FMA towards a system ASC subtype - ASCT2. Between two subtypes, ASCT1 and ASCT2, the latter demonstrated overexpression in a variety of cancer cells and plays essential role for tumor growth and survival. Inhibitory effect of GPNA, a potent ASCT2 inhibitor, was compared to its close analog GA that is inactive towards ASCT2 (Fig. 5C). There was no apparent difference between inhibition result of GPNA and GA and they could only reduce uptake of L-[^{18}F]FMA up to 28% at 1 mM concentration. This result indicate that L-[^{18}F]FMA is not selective for ASCT2 and ASCT1.

Furthermore, since L-[^{18}F]FMA is a close analog of L-Ala, we compared the transport of L[^{18}F]FMA and L-[^{3}H]Ala to examine the effect of fluroalkyl chain on the transport mechanism. The results (Fig. 6) demonstrated that L-[^{18}F]FMA and L-[^{3}H]Ala had similar transport characteristics. While L-[^{3}H]Ala is more sensitive towards inhibitors of system A and system L, both tracers appear mainly transported via system ASC and they are not selective towards ASCT2. To quantitatively evaluate the involvement of ASCT1 and ASCT2 in L-[^{18}F]FMA uptake, more extensive transport assays are required such as transporter mRNA expression profiling for 9L glioma cells and studies in ASCT1/2 knock-down cell lines.

3.5. In vitro metabolism studies

We tested the stability of L-[^{18}F]FMA in 9L cells by measuring the metabolites after 0, 30, 60, 120 min (Fig.7). The HPLC result of L-[^{18}F]FMA in PBS for 2 h without incubating with 9L cells was used as the control. No metabolite other than L-[^{18}F]FMA itself was

found in 2 h. This suggests that L-[^{18}F]FMA is metabolically stable within 2 h after being transported into 9L cells. Additionally, protein incorporation of L-[^{18}F]FMA was examined in 9L cells. No significant incorporation of L-[^{18}F]FMA into protein was observed. The protein bound fraction of L-[^{18}F]FMA was < 0.5%, in contrast to L-[^{3}H]Ala, which had significant incorporation (78.9 ± 2.9 %) into protein after 2 h. These result indicate that L-[^{18}F]FMA remained in its native form and was not further metabolized after transported into tumor cells.

3.6. In vivo biodistribution studies

The in vivo biodistribution studies of L-[^{18}F]FMA was carried out in Fisher rats bearing 9L tumors. The distribution of radioactivity in tissues after intravenous injection of L-[^{18}F]FMA at selected time points is summarized in Table 3. Uptake of L-[^{18}F]FMA in tumor was very fast and reached maximum uptake within 30 min. Rapid clearance of radioactivity in blood, heart, lung, pancreas, spleen and liver was observed within the first 30 min. Apart from bone, other examined organs had continuously decreasing radioactivity after 30 min. Bone uptake increased as a function of time from 0.48 %ID/g at 2 min to 1.91 %ID/g at 2 h, indicating substantial defluorination occurred. Although tumor tissue uptake was not very high, an adequate tumor-to-background ratio was achieved after 30 min. At 1 h, tumor-to-blood and tumor-to-muscle, and tumor-to-brain ratios reached 1.9, 2.2 and 3.0 respectively. The discrepancy between in vitro and in vivo tumor uptake is possibly the result of competition from natural amino acids present in the blood circulation of animals. Total concentration of system ASC substrates, including alanine, serine and threonine, is over 1 mM in rat plasma. In conjunction with in vitro inhibition data, this suggests it is possible to reduce the uptake of L-[^{18}F]FMA by >80%. In comparison, the tumor uptake of [^{18}F]FACBC appears to be less susceptible to the presence of natural amino acids in the blood circulation. The reason might be that FACBC is transported via multiple amino acid transport systems; besides system ASC, system L also plays an important role in its transport, especially in acidic environment that tumor cells live in. The significance of this observation will require additional studies to fully clarify the mechanisms responsible for the tumor cell uptake of these amino acid based imaging agents.

Highest uptake of L-[^{18}F]FMA in normal tissues was in liver followed by kidney, suggesting excretion through both biliary and renal routes. L-[^{18}F]FMA had very low pancreatic uptake after 30 min (< 0.3% ID/g). This pattern of biodistribution is quite different from those of many other amino acid tracers, which are excreted mainly via renal route and have high pancreatic uptake. This may relate to distribution of system ASC in tissues of rats. Further studies will be required to find out the underlying mechanism.

3.7. Small animal PET imaging studies

Small animal PET imaging studies of L-[^{18}F]FMA were carried out in two rodent tumor models: rats bearing 9L tumors and transgenic mice bearing spontaneous M/tomND tumors. The latter is a transgenic mouse model with spontaneously generated mammary gland adenocarcinoma. The 2 h summed images from coronal sections (Fig. 8A and Fig. 9A) were selected for visualization. Time-activity curves generated by drawing region of interest for assessing kinetics were shown in Fig. 8B and Fig. 9B. Tumors were visualized with L-[^{18}F]FMA in both animal models. Uptake in tumors in both animal models quickly reached the peak with 10 to 20 min. High activity in the skeleton (sternum, ribs et al) and gut regions was observed. Bone uptake suggests that there is apparent defluorination, consistent to that observed in biodistribution studies by dissection method (Table 3). Imaging analysis showed that tumor-to-muscle ratio in rat bearing 9L tumor increased from 2.6 at 30 min to 3.8 at 120 min, in agreement with the results from biodistribution studies. During the same time period, this ratio in transgenic mouse had small decrease from 2.3 to 2.0.

4. Conclusions

Three new ^{18}F labeled alanine derivatives were prepared with good radiochemical purity, high enantiomeric purity and reasonable radiochemical yields. In vitro tumor cell uptake studies demonstrated that L-[^{18}F]FMA had a higher uptake than the corresponding D-isomer. The longer alkyl chain derivative, L-[^{18}F]FEA, showed a lower tumor cell uptake. L-[^{18}F]FMA showed the highest uptake, higher than that of FDG, in a variety of tumor cell lines. It appears that L-[^{18}F]FMA was metabolically stable and primarily transported via sodium dependent system ASC in vitro. In vivo imaging studies demonstrated that L-[^{18}F]FMA had a fast and clear accumulation in tumors. Data presented in this paper suggest that L-[^{18}F]FMA may be a potentially useful PET imaging agent targeting tumor with an upregulated ASC amino acid transporter.

Acknowledgments

Authors wish to thank Dr. George Belka, for providing transgenic mice used in this report. This work was supported in part by grants from Stand-Up 2 Cancer grant (SU2C) and National Institutes of Health (CA-164490).

Abbreviations

ASC	alanine-serine-cysteine preferring amino acid transporter system
ASCT2	system ASC transporter subtype 2
BCH	2-amino-bicylo[2.2.1]heptane-2-carboxylic acid
FACBC	3-[^{18}F]fluoro-cyclobutyl-1-carboxylic acid
FC	flash chromatography
FDG	2-[^{18}F]fluoro-2-deoxy-D-glucose
FDOPA	6-[^{18}F]fluoro-3,4-dihydroxyphenylalanine
FET	O-(2-[^{18}F]fluoroethyl)-L-tyrosine
GA	L-γ-Glutamyl-anilide
GPNA	L-γ-Glutamyl-p-nitroanilide
HPLC	High performance liquid chromatography
HRMS	High-resolution mass spectrometry
L-FMA	3-(1-fluoromethyl)-L-alanine
L- FEA	3-(2-fluoroethyl)-L-alanine
MeAIB	*N*-methyl-α-aminoisobutyric acid IMT, 3-[^{123}I]Iodo-alpha-methyl-L-tyrosine
PBS	phosphate buffered saline
(SPE)	Solid-phase extraction
TCA	trichloroacetic acid
TFA	trifluoroacetic acid

References

1. McConathy J, Yu W, Jarkas N, Seo W, Schuster DM, Goodman MM. Radiohalogenated nonnatural amino acids as PET and SPECT tumor imaging agents. Med Res Rev. 2011 published online July 26. 10.1002/med.20250

2. McConathy J, Goodman MM. Non-natural amino acids for tumor imaging using positron emission tomography and single photon emission computed tomography. Cancer Metastasis Rev. 2008; 27:555–73. [PubMed: 18648909]
3. Plathow C, Weber WA. Tumor cell metabolism imaging. J Nucl Med. 2008; 49 (Suppl 2):43S–63S. [PubMed: 18523065]
4. Jager PL, Vaalburg W, Pruim J, de Vries EG, Langen KJ, Piers DA. Radiolabeled amino acids: basic aspects and clinical applications in oncology. J Nucl Med. 2001; 42:432–45. [PubMed: 11337520]
5. Okudaira H, Shikano N, Nishii R, Miyagi T, Yoshimoto M, Kobayashi M, et al. Putative Transport Mechanism and Intracellular Fate of Trans-1-Amino-3-18F-Fluorocyclobutanecarboxylic Acid in Human Prostate Cancer. J Nucl Med. 2011; 52:822–9. [PubMed: 21536930]
6. Asano Y, Inoue Y, Ikeda Y, Kikuchi K, Hara T, Taguchi C, et al. Phase I clinical study of NMK36: a new PET tracer with the synthetic amino acid analogue anti-[(18)F]FACBC. Ann Nucl Med. 2011; 25:414–8. [PubMed: 21409348]
7. Wang L, Qu W, Lieberman B, Ploessl K, Kung H. Synthesis and in vitro evaluation of 18F labeled tyrosine derivatives as potential positron emission tomography (PET) imaging agents. Bioorg Med Chem Lett. 2010; 20:3482–5. [PubMed: 20529679]
8. Popperl G, Kreth FW, Herms J, Koch W, Mehrkens JH, Gildehaus FJ, et al. Analysis of 18F-FET PET for grading of recurrent gliomas: is evaluation of uptake kinetics superior to standard methods? J Nucl Med. 2006; 47:393–403. [PubMed: 16513607]
9. Lee TS, Ahn SH, Moon BS, Chun KS, Kang JH, Cheon GJ, et al. Comparison of 18F-FDG, 18F-FET and 18F-FLT for differentiation between tumor and inflammation in rats. Nucl Med Biol. 2009; 36:681–6. [PubMed: 19647174]
10. Langen KJ, Hamacher K, Weckesser M, Floeth F, Stoffels G, Bauer D, et al. O-(2-[18F]fluoroethyl)-L-tyrosine: uptake mechanisms and clinical applications. Nucl Med Biol. 2006; 33:287–94. [PubMed: 16631076]
11. Ganapathy V, Thangaraju M, Prasad P. Nutrient transporters in cancer: relevance to Warburg hypothesis and beyond. Pharmacol Ther. 2009; 121:29–40. [PubMed: 18992769]
12. Hyde R, Taylor PM, Hundal HS. Amino acid transporters: roles in amino acid sensing and signalling in animal cells. Biochem J. 2003; 373:1–18. [PubMed: 12879880]
13. Fuchs BC, Bode BP. Amino acid transporters ASCT2 and LAT1 in cancer: partners in crime? Semin Cancer Biol. 2005; 15:254–66. [PubMed: 15916903]
14. Fan X, Ross DD, Arakawa H, Ganapathy V, Tamai I, Nakanishi T. Impact of system L amino acid transporter 1 (LAT1) on proliferation of human ovarian cancer cells: a possible target for combination therapy with anti-proliferative aminopeptidase inhibitors. Biochem Pharmacol. 2010; 80:811–8. [PubMed: 20510678]
15. Sakata T, Ferdous G, Tsuruta T, Satoh T, Baba S, Muto T, et al. L-type amino-acid transporter 1 as a novel biomarker for high-grade malignancy in prostate cancer. Pathol Int. 2009; 59:7–18. [PubMed: 19121087]
16. Singhal T, Narayanan TK, Jain V, Mukherjee J, Mantil J. 11C-L-methionine positron emission tomography in the clinical management of cerebral gliomas. Mol Imaging Biol. 2008; 10:1–18. [PubMed: 17957408]
17. Langen KJ, Muhlensiepen H, Holschbach M, Hautzel H, Jansen P, Coenen HH. Transport mechanisms of 3-[123I]iodo-a-methyl-L-tyrosine in a human glioma cell line: comparison with [3H-methyl]-L-methionine. J Nucl Med. 2000; 41:1250–5. [PubMed: 10914918]
18. Fueger BJ, Czernin J, Cloughesy T, Silverman DH, Geist CL, Walter MA, et al. Correlation of 6-18F-fluoro-L-dopa PET uptake with proliferation and tumor grade in newly diagnosed and recurrent gliomas. J Nucl Med. 2010; 51:1532–8. [PubMed: 20847166]
19. Minn H, Kauhanen S, Seppanen M, Nuutila P. 18F-FDOPA: a multiple-target molecule. J Nucl Med. 2009; 50:1915–8. [PubMed: 19910423]
20. Tolvanen T, Nagren K, Yu M, Sutinen E, Havu-Auren K, Jyrkkio S, et al. Human radiation dosimetry of [11C]MeAIB, a new tracer for imaging of system A amino acid transport. Eur J Nucl Med Mol Imaging. 2006; 33:1178–84. [PubMed: 16721566]

21. Sutinen E, Jyrkkio S, Alanen K, Nagren K, Minn H. Uptake of [N-methyl-11C]alpha-methylaminoisobutyric acid in untreated head and neck cancer studied by PET. Eur J Nucl Med Mol Imaging. 2003; 30:72–7. [PubMed: 12483412]
22. Schmall B, Conti PS, Alauddin MM. Synthesis of [11C-methyl]-alpha-aminoisobutyric acid (AIB). Nucl Med Biol. 1996; 23:263–6. [PubMed: 8782235]
23. Schuster DM, Savir-Baruch B, Nieh PT, Master VA, Halkar RK, Rossi PJ, et al. Detection of recurrent prostate carcinoma with anti-1-amino-3-18F-fluorocyclobutane-1-carboxylic acid PET/CT and 111In-capromab pendetide SPECT/CT. Radiology. 2011; 259:852–61. [PubMed: 21493787]
24. Yu W, Williams L, Camp V, Olson J, Goodman M. Synthesis and biological evaluation of anti-1-amino-2-[18F]fluoro-cyclobutyl-1-carboxylic acid (anti-2-[18F]FACBC) in rat 9L gliosarcoma. Bioorg Med Chem Lett. 2010; 20:2140–3. [PubMed: 20207538]
25. Oka S, Okudaira H, Yoshida Y, Schuster DM, Goodman MM, Shirakami Y. Transport mechanisms of trans-1-amino-3-fluoro[1-(14)C]cyclobutanecarboxylic acid in prostate cancer cells. Nucl Med Biol. 2011
26. Fuchs BC, Finger RE, Onan MC, Bode BP. ASCT2 silencing regulates mammalian target-of-rapamycin growth and survival signaling in human hepatoma cells. Am J Physiol Cell Physiol. 2007; 293:C55–63. [PubMed: 17329400]
27. Nakanishi T, Tamai I. Solute carrier transporters as targets for drug delivery and pharmacological intervention for chemotherapy. J Pharm Sci. 2011; 100:3731–50. [PubMed: 21630275]
28. Lee BH, Gerfen GJ, Miller MJ. Alternate syntheses of delta-N-hydroxy-L-ornithine derivatives and applications to the synthesis of rhodotorulic acid. J Org Chem. 1984; 49:2418–23.
29. Qu W, Zha Z, Ploessl K, Lieberman BP, Zhu L, Wise DR, et al. Synthesis of optically pure 4-fluoro-glutamines as potential metabolic imaging agents for tumors. J Am Chem Soc. 2011; 133:1122–33. [PubMed: 21190335]
30. Vaalburg W, Coenen HH, Crouzel C, Elsinga PH, Langstrom B, Lemaire C, et al. Amino acids for the measurement of protein synthesis in vivo by PET. Int J Rad Appl Instrum B. 1992; 19:227–37. [PubMed: 1601675]
31. Tsukada H, Sato K, Fukumoto D, Kakiuchi T. Evaluation of D-isomers of O-F-18-fluoromethyl, O-F-18-fluoroethyl and O-F-18-fluoropropyl tyrosine as tumour imaging agents in mice. Eur J Nucl Med Mol Imaging. 2006; 33:1017–24. [PubMed: 16699766]
32. Bauwens M, Lahoutte T, Kersemans K, Gallez C, Bossuyt A, Meltens J. Comparison of the uptake of [I-123/125]-2-iodo-D-tyrosine and [I-123/125]-2-iodo-L-tyrosine in R1M rhabdomyosarcoma cells in vitro and in R1M tumor-bearing Wag/Rij rats in vivo. Nucl Med Biol. 2006; 33:735–41. [PubMed: 16934692]
33. Wang L, Lieberman BP, Plossl K, Qu W, Kung HF. Synthesis and comparative biological evaluation of L- and D-isomers of 18F-labeled fluoroalkyl phenylalanine derivatives as tumor imaging agents. Nucl Med Biol. 2011; 38:301–12. [PubMed: 21492778]
34. Utsunomiya-Tate N, Endou H, Kanai Y. Cloning and functional characterization of a system ASC-like Na+-dependent neutral amino acid transporter. J Bio Chem. 1996; 271:14883–90. [PubMed: 8662767]
35. Esslinger CS, Cybulski KA, Rhoderick JF. N-gamma-aryl glutamine analogues as probes of the ASCT2 neutral amino acid transporter binding site. Bioorg Med Chem. 2005; 13:1111–8. [PubMed: 15670919]
36. Scharff R, Wool IG. Effect of diabetes on the concentration of amino acids in plasma and heart muscle of rats. Biochem J. 1966; 99:173–8. [PubMed: 5965335]
37. Martarello L, McConathy J, Camp VM, Malveaux EJ, Simpson NE, Simpson CP, et al. Synthesis of syn- and anti-1-amino-3-[18F]fluoromethyl-cyclobutane-1-carboxylic acid (FMACBC), potential PET ligands for tumor detection. J Med Chem. 2002; 45:2250–9. [PubMed: 12014963]
38. Schoenherr RM, Kelly-Spratt KS, Lin C, Whiteaker JR, Liu T, Holzman T, et al. Proteome and transcriptome profiles of a Her2/Neu-driven mouse model of breast cancer. Proteomics Clin Appl. 2011; 5:179–88. [PubMed: 21448875]

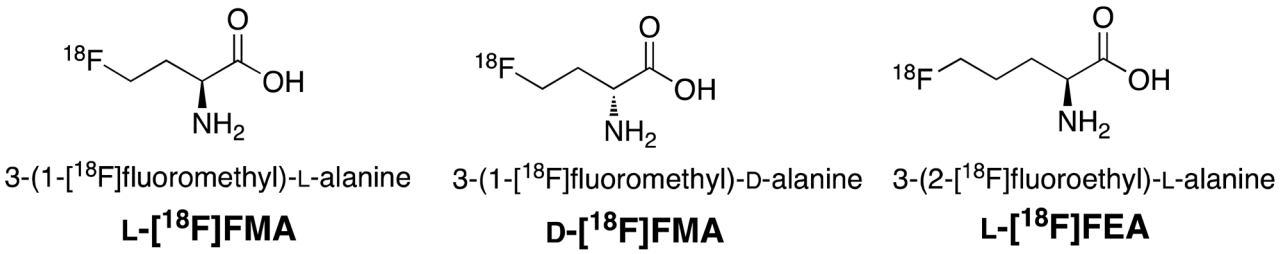

Fig. 1.
Chemical structures of new ^{18}F alanine derivatives.

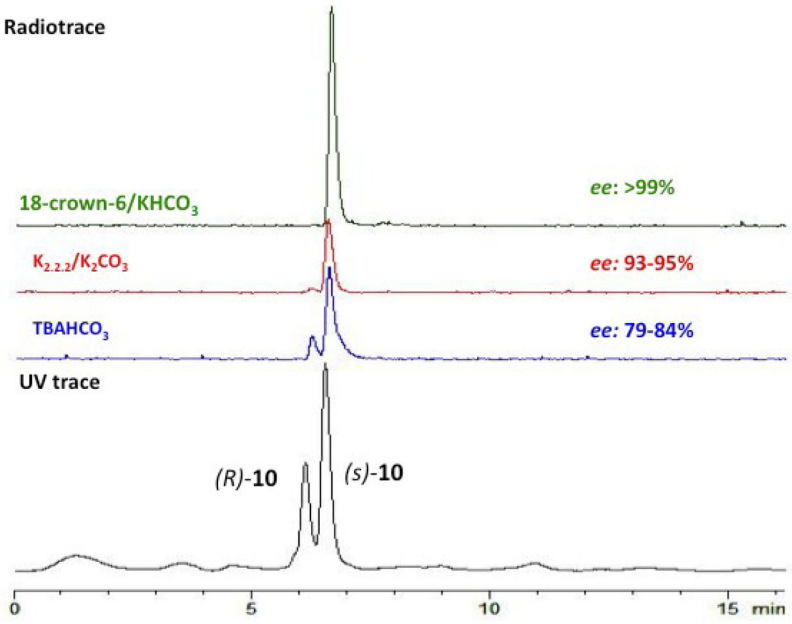

Fig. 2.

Effects of fluorination reagents and catalysts on the purity and yield of radiosynthesis of L-[^{18}F]FMA were evaluated using HPLC. Top three HPLC profile is the radiotrace of intermediate [^{18}F]**10**. Bottom HPLC profile (in Black) is the UV tracer of cold standard (*S*) and (*R*)-**10**.

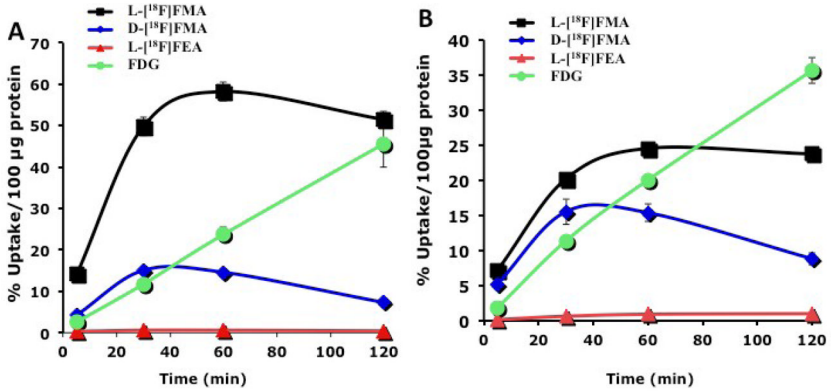

Fig. 3.

Time vs uptake of ^{18}F alanine derivatives into 9L (A) and PC-3 (B) are presented. A standard agent, FDG, was also measured in the same uptake conditions. It is important to note that the uptake of L-[18F]FMA is higher than that of FDG at 60 min. Uptake value are shown as % uptake/100 μg protein. Each point represents mean ± SD (n = 3).

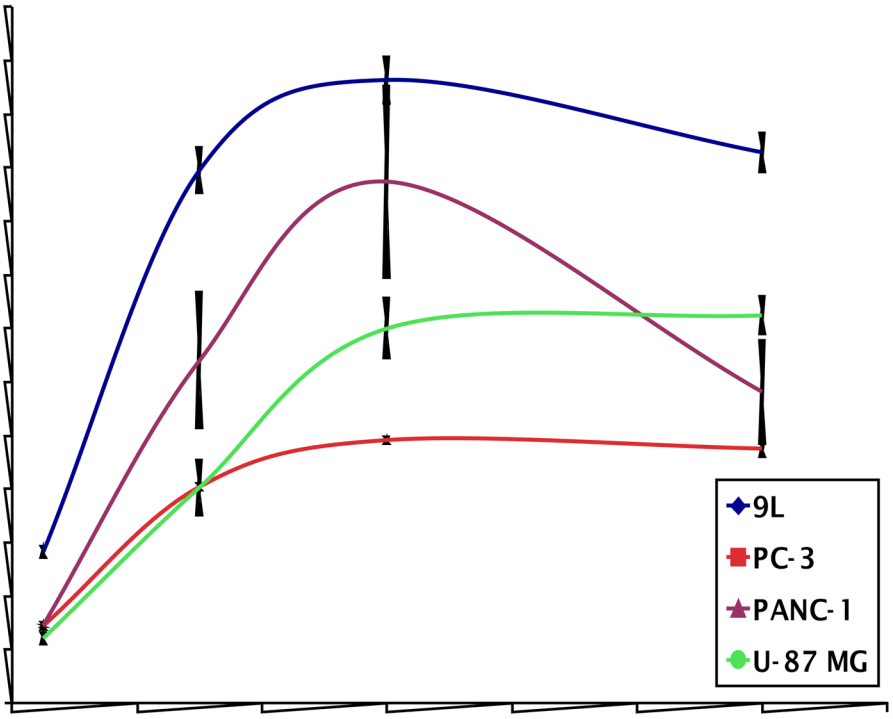

Fig. 4.

Time course of L-[^{18}F]FMA in various cancer cells was evaluated in four different tumor cells. Uptake value are represented as % uptake/100 μg protein. Each point represents mean ± SD (n = 3).

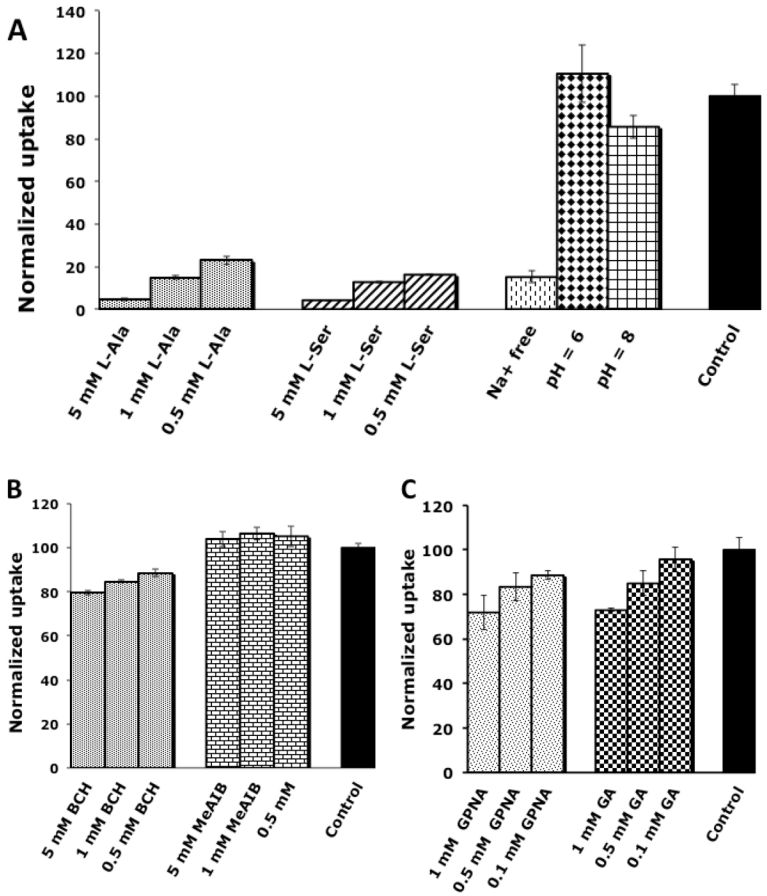

Fig. 5.

Transportation of L-[^{18}F]FMA in 9L glioma cells across tumor cells were evaluated in the presence of various amino acid transporter inhibitors. Uptake of L[^{18}F]FMA in presence of inhibitors for system ASC (A), A and L (B), and media free of Na+ and at different pH (A) were normalized to the uptake of L-[^{18}F]FMA in PBS solution (pH = 7.4) at 30 min. Data are expressed as mean ± SD (n = 3).

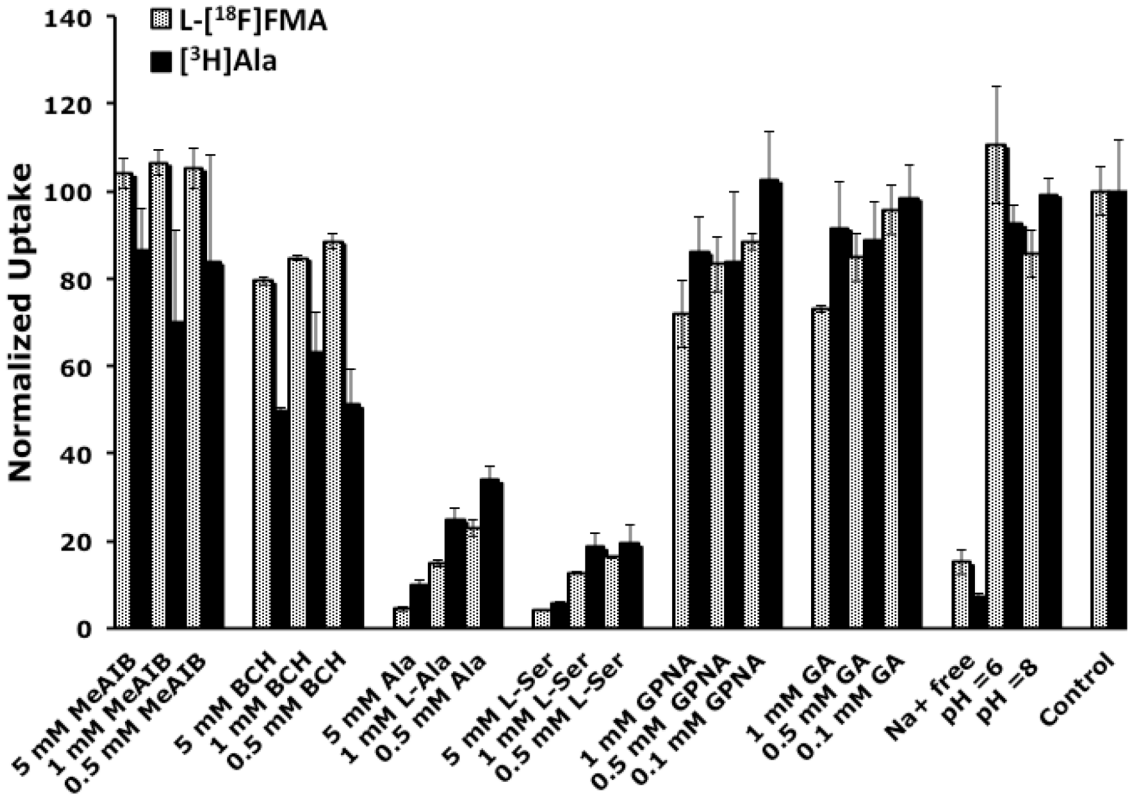

Fig. 6.

Comparison of tumor cell uptake of L-[^{18}F]FMA and [^{3}H]Ala in the presence of various inhibitors of amino acid transporter as well as in Na+ free and different pH buffers. Data are shown as mean ± SD (n = 3).

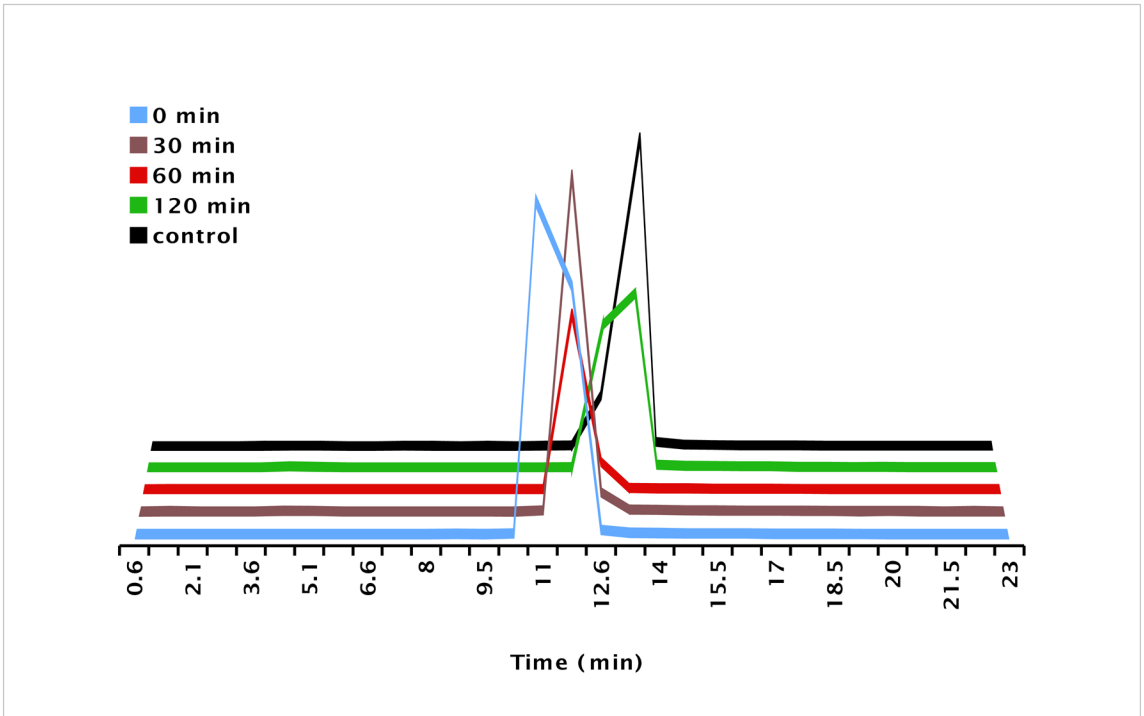

Fig. 7.
Metabolic stability of L-[^{18}F]FMA in 9L glioma cells was measured by HPLC.

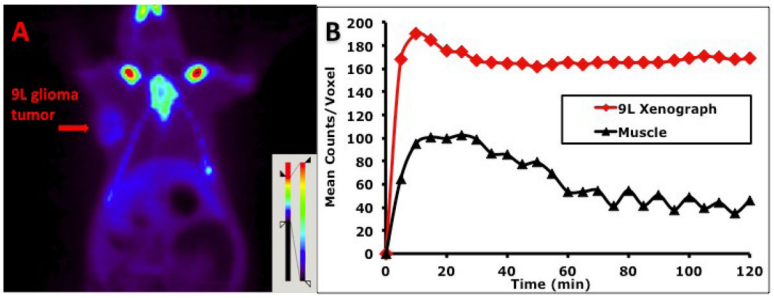

Fig. 8.

Small animal PET imaging of L-[^{18}F]FMA in Fisher rat bearing 9L tumor model was performed: (A) Color-coded PET image from summed 2 h data in coronal view. The arrowhead points to the 9L tumor. (B) Time activity curves in 9L tumors and muscle.

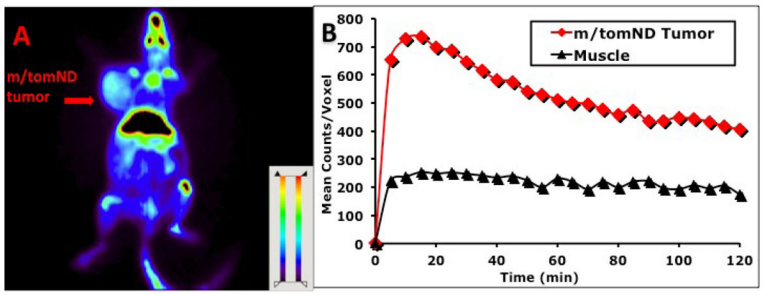

Fig. 9.

Small animal PET imaging of L-[^{18}F]FMA in transgenic mice bearing spontaneously generated mammary gland tumor (or m/tomND tumor) was performed: (A) Color-coded PET image from summed 2 h data in coronal view. The arrowhead points to the m/tomND tumor. (B) Time activity curves in m/tomND tumor and muscle.

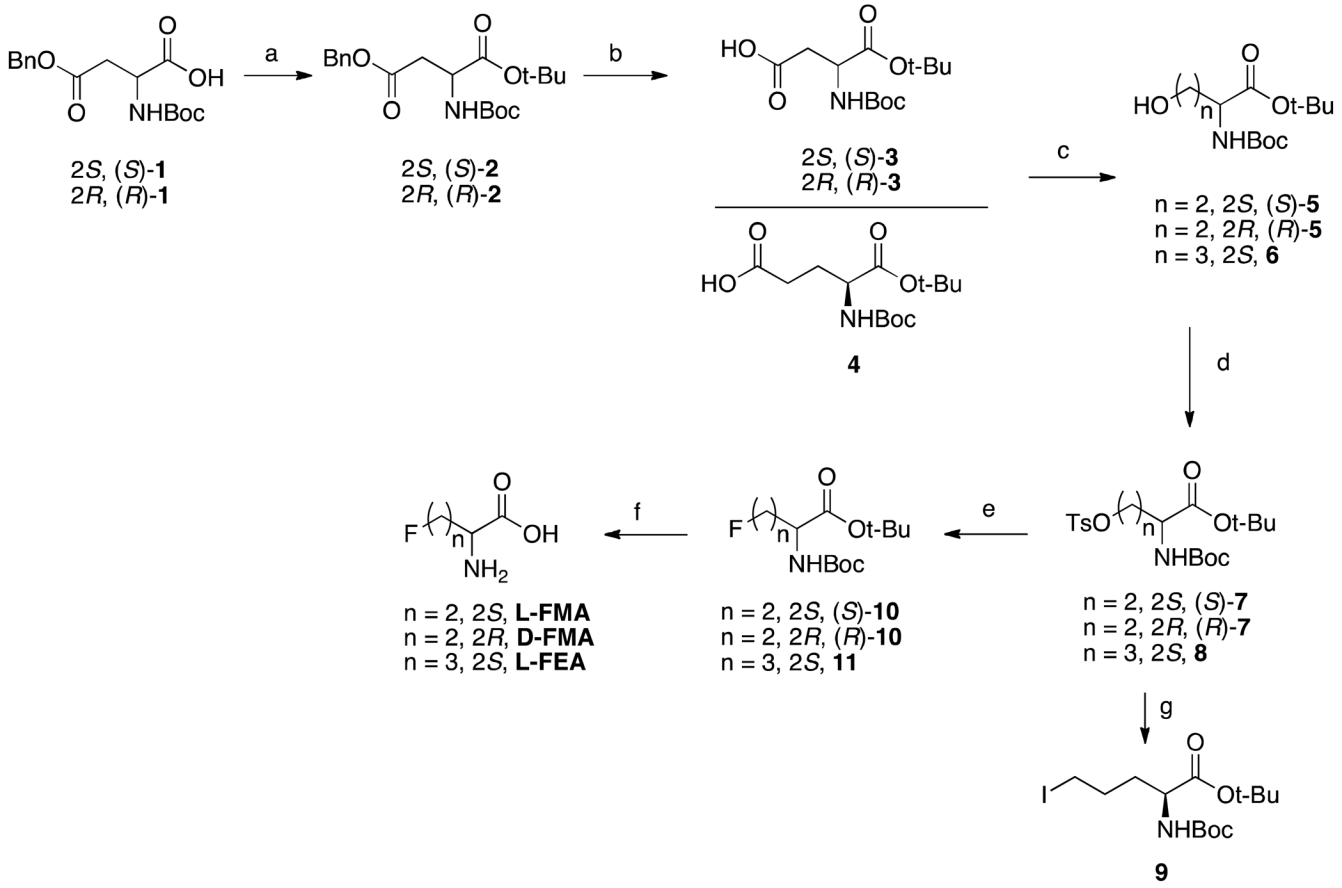

Scheme 1.

Synthesis of labeling precursors and standards for FMA and FEA. Reagents and conditions: (a) *tert*-butyl 2,2,2-trichloroacetamidate, $BF_3.Et_2O$, rt; (b) 10% Pd/C, H_2, rt; (c) i. ethyl chloroformate, Et_3N, −5 ~ −10 °C; ii. $NaBH_4$, H_2O, 0 °C to rt; (d) TsCl, Et_3N, DMAP, CH_2Cl_2, 0 °C to rt; (e) TASF, $Et_3N(HF)_3$, THF, CH_2Cl_2, 60 °C; (f) TFA, 0 °C to rt; (g) NaI, acetone, 60 °C.

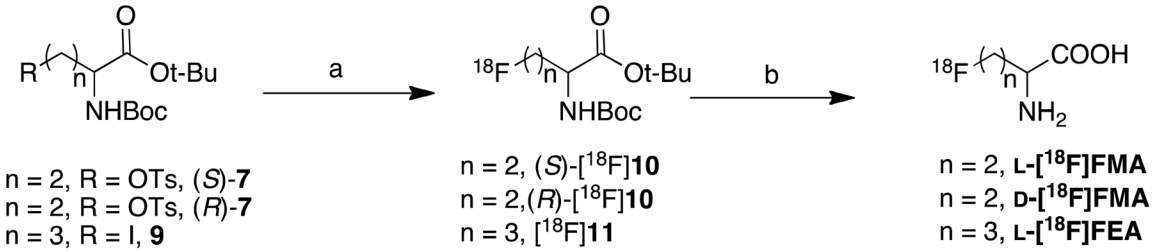

Scheme 2.

Radiolabeling of FMA and FEA. Reagents and conditions: (a) 18-Crown-6/$KHCO_3$/ K[18F]F, for L- and D-[18F]FMA: DMSO, 80, 15 min; for L-[^{18}F]FEA: CH^3CN, 60, 10 min; (b) TFA, 60, 10 min.

Table 1

Summary of radiolabeling of [^{18}F]FMA and [^{18}F]FEA *

Tracer	Synthesis Time (min)	RCY (%)	RCP (%)	Enantiomeric Purity (ee, %)
L-[^{18}F]FMA	63 – 74	18 – 34	> 99	> 99
D-[^{18}F]FMA	61 – 75	22 –24	> 99	> 99
L- [^{18}F]FEA	60 – 74	7 – 9	> 99	> 99

* Data was obtained from 3 to 6 experiments under the labeling conditions described in scheme 2

Table 2

Effect of solvent and temperature on radiofluorination of L-[^{18}F]FMA

	Temperature ( )	Solvent	RCP (%)	RCY (%)
1	70	ACN	>99	27
2	70	DMSO	>99	30
3	80	ACN	>99	31
4	50	DMSO	>99	36
5	90	ACN	>99	25
6	90	DMSO	>99	35
7	100	ACN	92	15
8	100	DMSO	96	14

Table 3

Biodistribution result of L-[^{18}F]FMA in Fisher rats bearing 9L tumors after intravenous injection[a]

Organ	2 min	30 min	60 min	120 min
Blood	0.76 ± 0.04	0.39 ± 0.04	0.20 ± 0.02	0.09 ± 0.01
Heart	1.01 ± 0.06	0.29 ± 0.03	0.16 ± 0.02	0.09 ± 0.01
Muscle	0.18 ± 0.04	0.27 ± 0.03	0.18 ± 0.02	0.09 ± 0.01
Lung	1.32 ± 0.09	0.45 ± 0.02	0.26 ± 0.02	0.17 ± 0.02
Kidney	1.76 ± 0.25	1.32 ± 0.14	0.94 ± 0.06	0.51 ± 0.09
Pancreas	1.98 ± 0.44	0.30 ± 0.03	0.21 ± 0.06	0.16 ± 0.08
Spleen	1.76 ± 0.12	0.42 ± 0.04	0.26 ± 0.06	0.13 ± 0.02
Liver	2.48 ± 0.28	1.32 ± 0.12	1.21 ± 0.12	0.68 ± 0.10
Skin	0.27 ± 0.10	0.27 ± 0.04	0.20 ± 0.01	0.11 ± 0.02
Brain	0.12 ± 0.01	0.14 ± 0.01	0.13 ± 0.01	0.12 ± 0.01
Bone	0.48 ± 0.06	1.07 ± 0.36	1.70 ± 0.31	1.91 ± 0.58
Tumor	0.58 ± 0.09	0.54 ± 0.07	0.39 ± 0.08	0.34 ± 0.06
Uptake ratio				
Tumor-to-blood	0.8 ± 0.1	1.4 ± 0.2	1.9 ± 0.4	3.8 ± 0.8
Tumor-to-muscle	3.2 ± 0.9	2.0 ± 0.3	2.2 ± 0.5	3.8 ± 0.8
Tumor-to-brain	4.8 ± 0.9	3.9 ± 0.6	3.0 ± 0.7	2.8 ± 0.6

[a]Values are reported as mean (% ID/g) ± SD; n = 6 rats per time point.